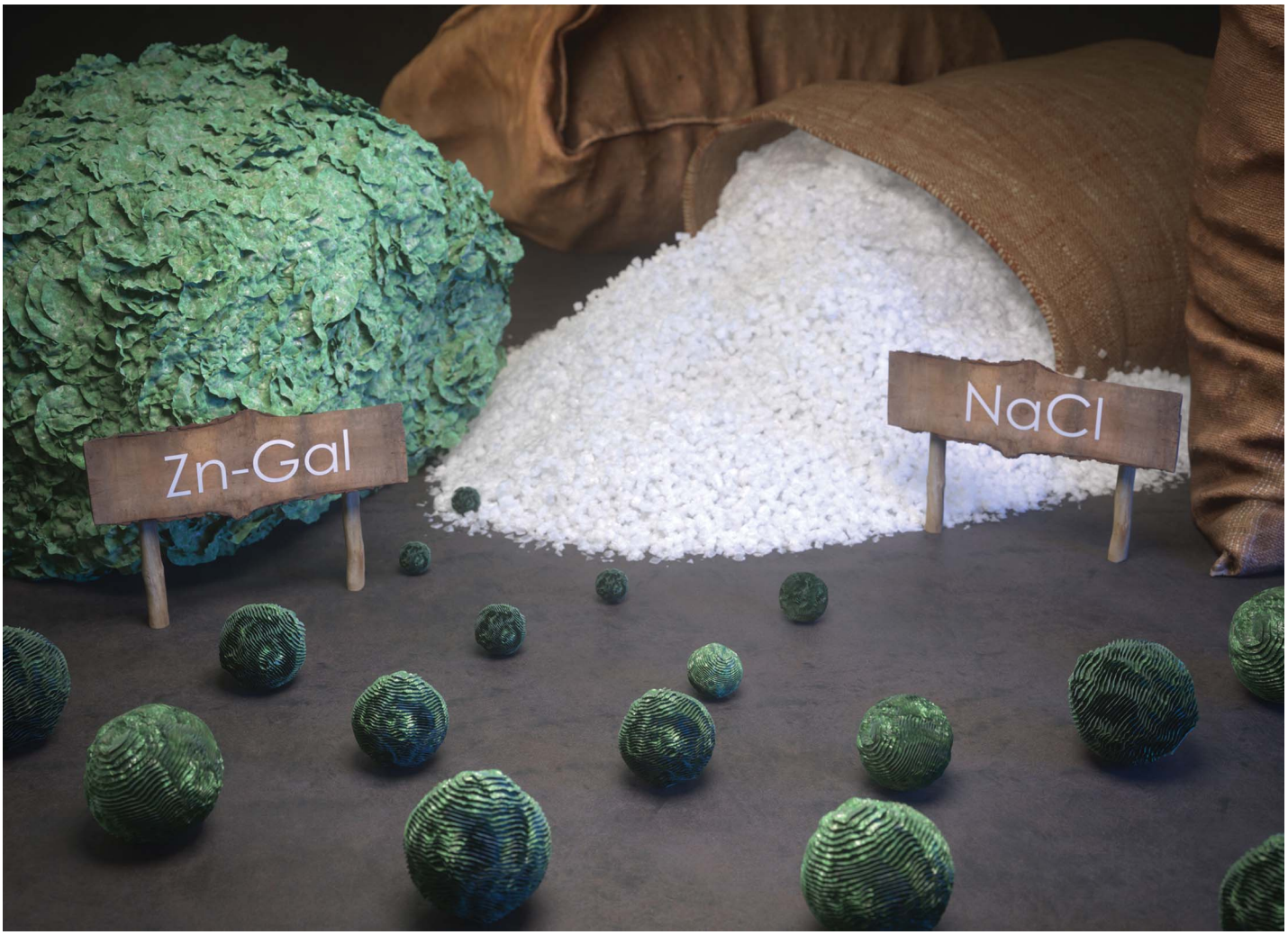

Highlighting a nanoengineering study on heterogeneous catalysts from Professor Seung Uk Son's laboratory, Department of Chemistry, Sungkyunkwan University, Korea.

Morphology engineering of 2D Zn-catalysts to wrinkled particles using NaCl microcrystals: enhanced recyclability for the synthesis of poly(caprolactone)s

Wrinkled Zn-gallate nanoparticles (W-Zn-Gal NP) were synthesized using micron-sized NaCl crystals as morphology-directing agents. In contrast to control Zn-Gal plate structures, which showed only moderate catalytic activity and limited recyclability due to easy aggregation and structural cleavage, W-Zn-Gal NP exhibited superior catalytic efficiency and improved recyclability in the ring-opening polymerization of ε-caprolactone to poly(caprolactone).

Image reproduced by permission of Seung Uk Son from *J. Mater. Chem. A*, 2025, **13**, 23439.

As featured in:

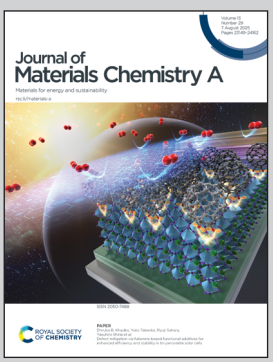

See Seung Uk Son *et al.*, *J. Mater. Chem. A*, 2025, **13**, 23439.

ROYAL SOCIETY OF CHEMISTRY

rsc.li/materials-a

Registered charity number: 207890

Journal of Materials Chemistry A

ROYAL SOCIETY OF CHEMISTRY

COMMUNICATION

View Article Online
View Journal | View Issue

Check for updates

Cite this: *J. Mater. Chem. A*, 2025, **13**, 23439

Received 17th March 2025
Accepted 2nd June 2025

DOI: 10.1039/d5ta02177d

rsc.li/materials-a

Morphology engineering of 2D Zn-catalysts to wrinkled particles using NaCl microcrystals: enhanced recyclability for the synthesis of poly(caprolactone)s†

Seram Kim,‡ Jong Doo Lee ‡ and Seung Uk Son *

Zn-gallate nanoparticles with a wrinkled surface structure (W-Zn-Gal NP) were engineered using micron-sized NaCl crystals as morphology-guiding materials. While control Zn-Gal plates exhibited moderate catalytic activity and poor recyclability, due to the facile plate–plate packing and facile cleavage into pieces, W-Zn-Gal NP showed excellent catalytic performance and enhanced recyclability in the ring-opening polymerization of ε-caprolactone to poly(caprolactone).

Heterogeneous catalysts are critical components for sustainable polymer chemistry.[1] For example, efficient heterogeneous Lewis acid catalysts are required for the synthesis of biodegradable plastics[2] and the reuse of plastic waste.[3] To utilize molecular catalytic activities, the complexation of metals with ligands bearing multiple coordination sites is an efficient method for obtaining insoluble materials.[4] In the synthesis of metal–ligand coordination polymers, insoluble materials with 2D structural motifs are often obtained.[5] While heterogeneous catalysts with 2D morphologies can efficiently utilize catalytic sites, due to their surface-rich character, their physical instability can be a challenge for use as heterogeneous catalytic materials.[6]

Gallic acid is a natural compound with multiple coordination sites, such as hydroxy and carboxylic acid groups, for binding to transition metals.[7] Recently, insoluble coordination polymers have been prepared by reacting zinc salts with gallic acid.[8] The resulting Zn-gallate (Zn-Gal) materials exhibited a 2D structural motif and formed aggregates through plate–plate packing (Fig. 1). The packing resulted in reduced catalytic activities due to the limited diffusion of substrates toward the catalytic sites on the surface of Zn-Gal plates.[9]

Although Zn-Gal plates exhibited excellent catalytic activity as a Lewis acid catalyst for sustainable chemistry, they were easily fragmented into pieces during catalytic reactions (Fig. 1).[8] As a result, separating the Zn-Gal catalysts from the reaction mixture and products was unsuccessful.[8] To enable the recovery and recycling of Zn-Gal catalysts, further morphological engineering of the catalysts is required.

NaCl is one of the most common chemicals in everyday life and has been utilized in materials chemistry.[10] In particular, there have been studies on the morphological engineering of functional materials using NaCl crystals.[11] One of the key advantages of NaCl crystals as a morphology-guiding material is that they can be easily removed from functional materials through simple water washing. In this regard, we have attempted to engineer the morphology of Zn-Gal plates using NaCl crystals.

Recently, due to environmental issues, biodegradable polymers have gained great attention from scientists.[12] Polyesters have been studied as promising biodegradable polymers due to the gradual hydrolysis of ester bonds.[13] For example, poly(-caprolactone) (PCL) has been regarded as a biodegradable polyester.[14] PCL has been synthesized through the ring-opening polymerization of ε-caprolactone (ε-CL).[14,15]

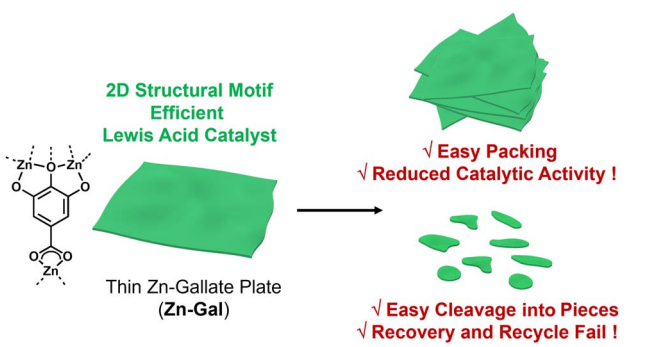

Fig. 1 Challenges associated with the catalytic applications of zinc-gallate (Zn-Gal) plates.

Department of Chemistry, Sungkyunkwan University, Suwon 16419, Korea. E-mail: sson@skku.edu

† Electronic supplementary information (ESI) available: Experimental procedures, additional SEM images, and additional characterization data of catalysts and PCLs. See DOI: https://doi.org/10.1039/d5ta02177d

‡ These authors contributed equally to this work.

While various homogeneous Lewis acid catalysts including zinc compounds such as zinc acetate, zinc nitrate, and zinc chloride and non-zinc catalysts such as Ti, Sn, and lanthanide complexes have been studied for the synthesis of PCL,[14] recyclable heterogeneous catalysts are rare.[2,15] While the Zn or Sn complexes grafted onto solid supports such as polystyrene and halloysite have been studied as heterogeneous catalytic systems,[2,15b] their recyclability has not been clarified. While microporous organic polymers bearing Zn-poly(acrylic acid) were successful as recyclable heterogeneous catalysts, their preparation was not simple and involved significant synthetic effort.[15a] In this regard, further exploration for the efficient heterogeneous Lewis acid catalysts is required for the synthesis of PCL. In this work, we report the engineering of Zn-Gal nanoparticles with wrinkles (W-Zn-Gal NP) using micrometer-sized NaCl crystals (M-NaCl) as morphology-guiding materials and their catalytic performance in the synthesis of PCL.

Fig. 2 presents a synthetic scheme for W-Zn-Gal-NP using M-NaCl as a morphology-guiding material.

M-NaCl was prepared by recrystallizing NaCl through the dropwise addition of an aqueous NaCl solution into acetone. The reaction of zinc acetate with gallic acid in dimethylformamide in the presence of M-NaCl resulted in the formation of M-NaCl@Zn-Gal composite materials (Fig. S1 in the ESI†). After separating the composites from the reaction mixture by centrifugation, they were further ripened at 80 °C under vacuum overnight. After M-NaCl was etched from M-NaCl@Zn-Gal composites by simple water washing, the obtained materials were dried at 80 °C under vacuum to form W-Zn-Gal NP. As a control material, Zn-Gal was prepared by the same synthetic procedures as W-Zn-Gal NP without using M-NaCl.

While conventional NaCl particles have sizes of 309 ± 50 μm, scanning electron microscopy (SEM) images of M-NaCl showed sizes of 2.75 ± 0.40 μm (Fig. S2 in the ESI†). While Zn-Gal has a 2D structural motif to form very thin plates,[16] SEM and transmission electron microscopy (TEM) showed large aggregates of 2D materials that were disassembled to small plates (Fig. 3a–c, g and S3 in the ESI†). In comparison, the low magnification SEM images of W-Zn-Gal NP revealed very uniform particles with sizes of 671 ± 92 nm (Fig. 3d and S2 in the ESI†).

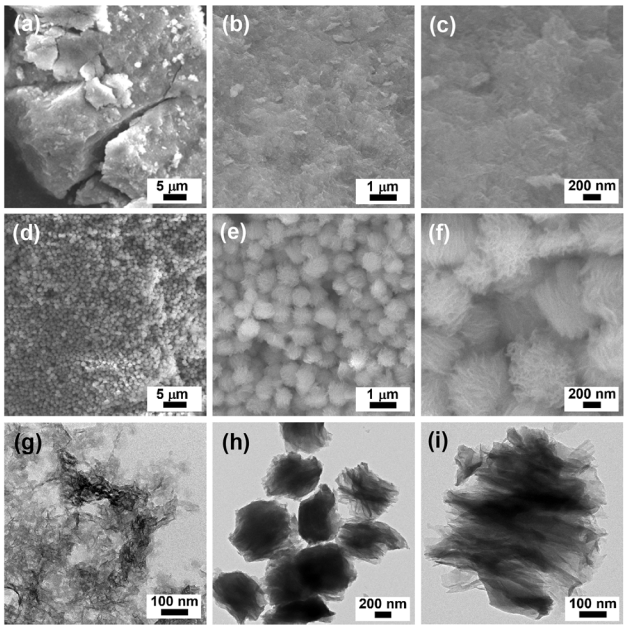

Fig. 3 SEM images of (a–c) Zn-Gal and (d–f) W-Zn-Gal NP. TEM images of (g) Zn-Gal and (h and i) W-Zn-Gal NP.

The careful investigation by SEM and TEM studies indicated that W-Zn-Gal NP particles have intriguing wrinkled surface structures (Fig. 3e, f, h and i). It can be speculated that the wrinkles of W-Zn-Gal NP were formed through the etching of M-NaCl crystals and the successive shrinkage of remaining Zn-Gal plates during the drying process. SEM and TEM analysis of the intermediate materials indicated that the M-NaCl crystals in M-NaCl@Zn-Gal split into smaller crystals during etching, leading to the formation of submicrometer-sized W-Zn-Gal particles (Fig. S1 in the ESI†). When conventional NaCl crystals were used instead of M-NaCl, similarly wrinkled Zn-Gal materials were obtained; however, the material quality was relatively poor (Fig. S4 in the ESI†). Energy dispersive X-ray spectroscopy (EDS)-based elemental mapping studies indicated that the Zn-Gal materials were loaded onto M-NaCl in M-NaCl@Zn-Gal and that the M-NaCl crystals were etched away in W-Zn-Gal NP (Fig. S5 in the ESI†).[17]

The chemical structures of Zn-Gal and W-Zn-Gal NP were evaluated by various techniques. The powder X-ray diffraction (PXRD) pattern of W-Zn-Gal NP indicated that M-NaCl was completely etched from M-NaCl@Zn-Gal composites and matched well with that of Zn-Gal (Fig. 4a). In addition, the main XRD peaks at 2θ of 10.06° indicated 2D structures of Zn-Gal and W-Zn-Gal with an interplanar distance of 8.8 Å.[16]

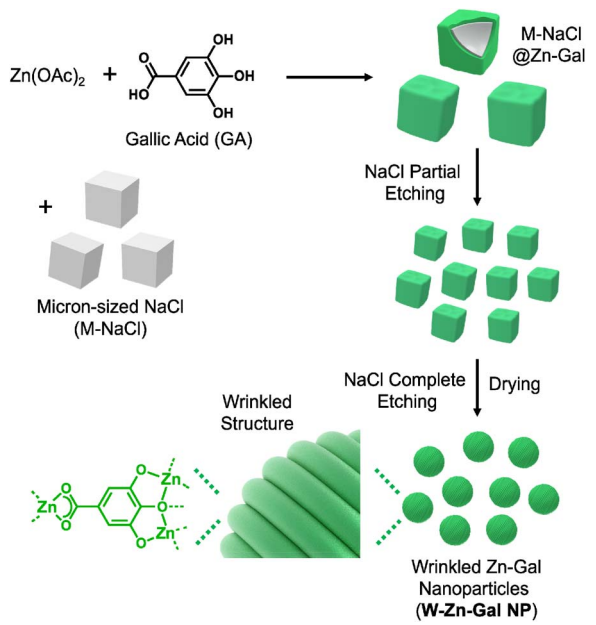

Fig. 2 A synthetic scheme for W-Zn-Gal NP.

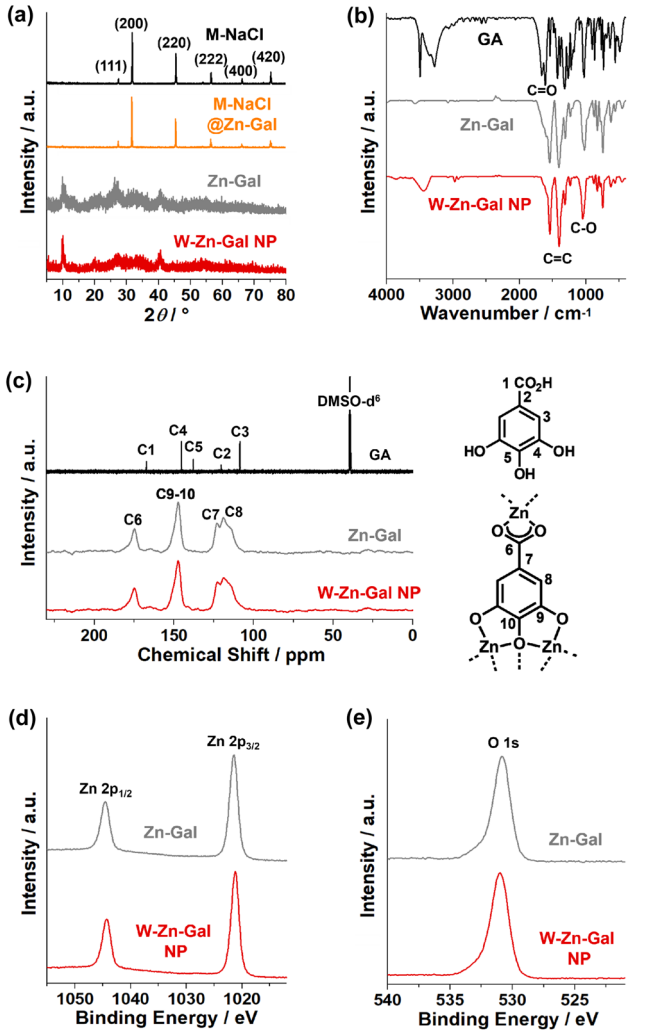

Fig. 4 (a) PXRD patterns of M-NaCl, M-NaCl@Zn-Gal, Zn-Gal, and W-Zn-Gal NP. (b) IR and (c) solution/solid state ^{13}C NMR spectra of gallic acid (GA), Zn-Gal, and W-Zn-Gal NP. (d) XPS Zn 2p orbital peaks and (e) O 1s orbital peaks of Zn-Gal and W-Zn-Gal NP.

While the infrared (IR) absorption spectrum of gallic acid (GA) showed the C=O vibration peak of carboxylic acid group at 1671 cm^{-1},[18] this peak was not observed in Zn-Gal and W-Zn-Gal-NP, indicating the formation of Zn-η^2 carboxylate species (Fig. 4b). The aromatic C=C vibration peaks of GA appeared at 1611 and 1420 cm^{-1},[18] which slightly shifted to 1546 and 1408 cm^{-1} in the IR spectra of Zn-Gal and W-Zn-Gal NP. In addition, the C=O vibration peak of GA at 1302 cm^{-1} shifted to 1026 cm^{-1} through Zn coordination to the hydroxyl groups of GA.[18] The IR peak at 3438 cm^{-1} of W-Zn-Gal NP is attributable to adsorbed water.

By inductively coupled plasma-atomic emission spectroscopy (ICP-AES), the Zn contents of Zn-Gal and W-Zn-Gal NP were analyzed to be 5.73 and 5.14 mmol Zn per g, respectively. Thermogravimetric analysis (TGA) indicated that W-Zn-Gal NP is more thermally stable up to 541 °C compared to Zn-Gal (204 °C) (Fig. S6 in the ESI†).

Solid state ^{13}C nuclear magnetic resonance (NMR) spectra of Zn-Gal and W-Zn-Gal NP exhibited ^{13}C peaks corresponding to carboxylates, phenolate carbons adjacent to oxygens, and other aromatic carbons at 175, 147, and 116–123 ppm, respectively, indicating that gallates were successfully incorporated into the materials (Fig. 4c). X-ray photoelectron spectroscopy (XPS) of Zn-Gal and W-Zn-Gal NP showed the Zn $2p_{1/2}$ and $2p_{3/2}$ orbital peaks at 1044.4 and 1021.2 eV, respectively, indicating that the Zn species have Zn(II) oxidation states (Fig. 4d).[19] In addition, the O 1s orbital peaks of Zn-gallate species in Zn-Gal and W-Zn-Gal-NP were observed at 530.8 eV, matching well with those of Zn-coordinated oxygens reported in the literature (Fig. 4e).[20]

Next, we studied the catalytic performance of W-Zn-Gal NP for the ring-opening polymerization of ε-CL to PCL, compared to Zn-Gal. Table 1 and Fig. S7, S8 in the ESI† summarize the results.

Water was used as an initiator for the ring-opening polymerization of ε-CL.[21] The hydroxy group originated from water attacks the carbonyl group of ε-CL to generate an alkoxy moiety. The alkoxy group attacks the carbonyl group of another ε-CL to induce the formation of polymer chains. Finally, the terminal alkoxy group is quenched by a proton originating from water. In the absence of a catalyst, a 12% yield of PCL was obtained at 160 °C after 24 h (Entry 1 in Table 1).

In comparison, in the presence of W-Zn-Gal NP (1.00 mol% Zn), the reactions produced a 96% yield of PCL at 160 °C after 24 h (Entries 2–6 in Table 1). The absolute molecular weight ($M_{n\text{-NMR}}$) of PCL gradually increased to 5300 g mol^{-1} ($M_{n\text{-GPC}}$ of 9200 and PDI of 1.86). It can be noted that M_n values have been corrected using the following equation: $M_n = 0.56M_{n\text{-GPC}}$, for PCL based on the Mark–Houwink correction.[22]

The M_n of PCL could be controlled by adjusting the amount of initiator (water).[23] When the amount of initiator increased from 1.6 μL (ε-CL/initiator = 50) to 3.2 μL (ε-CL/initiator = 25), the $M_{n\text{-NMR}}$ of PCL decreased from 5300 to 4700 (Entry 7 in Table 1). In contrast, when the amount of initiator was reduced to 0.8 μL (ε-CL/initiator = 100), the $M_{n\text{-NMR}}$ of PCL significantly increased to 6500, due to the reduced number of the activated polymer chains (Entry 8 in Table 1).

When the amount of W-Zn-Gal NP was reduced from 1.00 mol% Zn to 0.500 mol% Zn, the yield of PCL decreased from 96% to 91% (Entry 9 in Table 1). When the reaction temperature was decreased from 160 °C to 140 and 120 °C, the yields of PCL dropped to 86 and 50%, respectively (Entries 10 and 11 in Table 1). Thus, the optimal reaction conditions were determined as follows: 1.00 mol% Zn, 1.6 μL H_2O, 160 °C, and 24 h.

Compared to W-Zn-Gal NP, Zn-Gal (1.00 mol% Zn) showed much lower activities, generating an 85% yield of PCL with $M_{n\text{-NMR}}$ of 3400 under the optimized reaction conditions (Entries 12–16 in Table 1). Moreover, Zn-Gal exhibited poor recyclability due to the difficulty in recovering the small plates (Entries 16–20 in Table 1; Fig. 5a and S3 in the ESI†). The catalytic activities of Zn-Gal sharply dropped to generate an 11% yield of PCL in the fifth reaction. For further control tests, Zn-Gal was treated with water and then dried, following the workup process used for W-Zn-Gal NP (Fig. S9 in the ESI†). While the resulting Zn-Gal(H_2O),

Table 1 Ring-opening polymerization of ε-CL to PCL catalyzed by W-Zn-Gal NP (A) and Zn-Gal (B)[a]

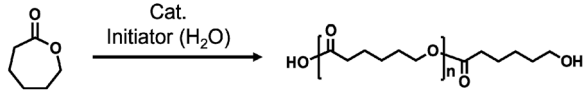

Entry	Cat.	Time (h)	Yield[b] (%)	$M_{n\text{-}NMR}$[c] (g mol^{-1})	$M_{n\text{-}GPC}$[d] (g mol^{-1})	PDI[e]
1	—	24	12(7)	900	—	—
2	A	3	37(35)	1400	—	—
3	A	6	71(64)	2700	—	—
4	A	12	93(80)	4700	—	—
5	A	18	96(89)	5200	—	—
6	A	24	96(91)	5300	9200	1.86
7[f]	A	24	91(89)	4700	9100	1.91
8[g]	A	24	90(89)	6500	10 300	1.94
9[h]	A	24	91(87)	3900	—	—
10[i]	A	24	86(85)	4100	—	—
11[j]	A	24	50(46)	2000	—	—
12	B	3	11(10)	700	—	—
13	B	6	24(22)	1100	—	—
14	B	12	50(41)	2300	—	—
15	B	18	71(55)	3800	—	—
16	B	24	85(73)	3400	8700	1.69
17[k]	B	24	81(61)	4000	9100	1.75
18[l]	B	24	81(57)	3500	6500	1.46
19[m]	B	24	59(36)	2600	4700	1.30
20[n]	B	24	11(7)	1100	2400	1.32
21[o]	A	24	98(91)	6300	11 900	1.95
22[p]	A	24	94(89)	7200	11 900	1.95
23[q]	A	24	96(87)	7200	12 900	1.86
24[r]	A	24	94(88)	6600	11 400	1.88

[a] Reaction conditions: ε-caprolactone (0.500 mL, 4.51 mmol), H_2O initiator (1.6 μL), W-Zn-Gal NP (A, 1.00 mol% Zn, 8.76 mg) or Zn-Gal (B, 1.00 mol% Zn, 6.98 mg), 160 °C. [b] Conversion yields based on ^{1}H NMR analysis and the isolated yields of PCL were given in parentheses. [c] M_n values based on ^{1}H NMR analysis. [d] M_n values based on GPC analysis. [e] Values obtained by GPC analysis. [f] 3.2 μL H_2O was used. [g] 0.8 μL H_2O was used. [h] 0.500 mol% Zn was used. [i] The reaction temperature of 140 °C was applied. [j] The reaction temperature of 120 °C was applied. [k] The catalyst B recovered from Entry 16 was used. [l] The catalyst B recovered from Entry 17 was used. [m] The catalyst B recovered from Entry 18 was used. [n] The catalyst B recovered from Entry 19 was used. [o] The catalyst A recovered from Entry 6 was used. [p] The catalyst A recovered from Entry 21 was used. [q] The catalyst A recovered from Entry 22 was used. [r] The catalyst A recovered from Entry 23 was used.

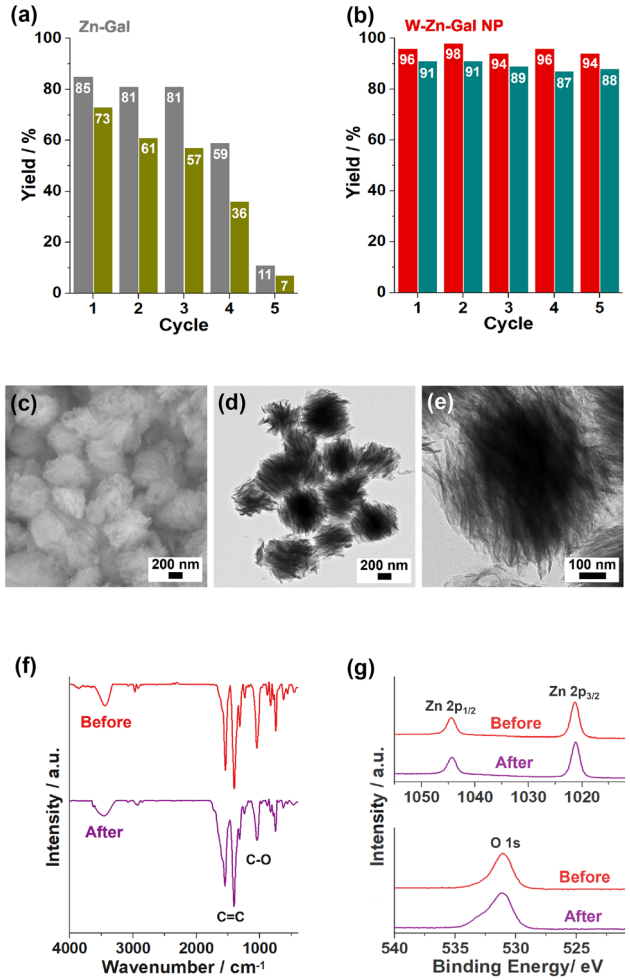

Fig. 5 Recyclability tests of (a) Zn-Gal and (b) W-Zn-Gal NP catalysts for the ring-opening polymerization of ε-CL to PCL (reaction conditions: ε-caprolactone (0.500 mL, 4.51 mmol), H_2O initiator (1.6 μL), W-Zn-Gal NP (1.00 mol% Zn) or Zn-Gal (1.00 mol% Zn), 24 h, and 160 °C). Conversion yields of CL and isolated yields of PCL were displayed. (c) SEM and (d and e) TEM images of W-Zn-Gal NP recovered after five successive reactions. (f) IR absorption and (g) XPS 2p orbital and O 1s orbital spectra of W-Zn-Gal NP recovered from the fifth run.

containing 5.13 mmol Zn per g, exhibited enhanced thermal stability (Fig. S10 in the ESI†) and improved catalytic activity in the first reaction due to the initiator role of adsorbed water,[24] it showed poor recyclability (Fig. S11 in the ESI†).

In comparison, W-Zn-Gal NP showed excellent recyclability in the five successive reactions, maintaining the yields of PCL in the range of 98–94% (isolated yields of 87–91%) (Entries 6 and 21–24 in Table 1 and Fig. 5b). The $M_{n\text{-NMR}}$ values of PCL slightly increased to 6300–7200 in the second to fifth reactions. The SEM and TEM studies of the recovered W-Zn-Gal NP indicated that its original wrinkle morphology was completely retained during the five successive runs (Fig. 5c–e). The IR, XPS, and PXRD analyses of W-Zn-Gal NP recovered after five successive runs indicated that the original chemical structures were retained (Fig. 5f, g and S12 in the ESI†). In addition, the surface area of the recovered W-Zn-Gal NP slightly decreased from 31 $m^2\ g^{-1}$ to 22 $m^2\ g^{-1}$ (Fig. S13 in the ESI†).

In conclusion, this work demonstrates the successful morphology engineering of heterogeneous Lewis acid catalysts using M-NaCl as a morphology-guiding material. While Zn-Gal plates have potential as a Lewis acid catalyst for the ring-opening polymerization of ε-CL to PCL, they showed poor recyclability. In comparison, the morphology-engineered W-Zn-Gal NP showed not only enhanced catalytic activities but also excellent recyclability as a heterogeneous catalytic system. We believe that the performance of various heterogeneous catalysts utilized in sustainable chemistry can be enhanced through NaCl-assisted morphology engineering.

Data availability

The data supporting this article have been included as part of the ESI†.

Author contributions

S. U. Son: conceptualization, supervision, writing original draft, and review & editing. S. Kim and J. D. Lee: investigation and formal analysis.

Conflicts of interest

There are no conflicts to declare.

Acknowledgements

This work was supported by the Carbon Upcycling Project for Platform Chemicals (No. RS-2022-NR068679) and by the National Research Foundation of Korea (NRF) grants (No. RS-2023-00208797) funded by the Korean government (MSIT).

Notes and references

1 (*a*) H. Wang, S. Huang and S. C. E. Tsang, *Chem. Commun.*, 2025, **61**, 1496–1508; (*b*) M. Chu, Q. Kang, P. Hu, Q. Zhang and J. Chen, *Chem. Eng. J.*, 2024, **496**, 154375; (*c*) L. O. Mark, M. C. Cendejas and I. Hermans, *ChemSusChem*, 2020, **13**, 5808–5836.

2 I. C. Howard, C. Hammond and A. Buchard, *Polym. Chem.*, 2019, **10**, 5894–5904.

3 H. Lv, F. Huang and F. Zhang, *Langmuir*, 2024, **40**, 5077–5089.

4 (*a*) Y.-S. Wei, M. Zhang, R. Zou and Q. Xu, *Chem. Rev.*, 2020, **120**, 12089–12174; (*b*) A. Herbst and C. Janiak, *CrystEngComm*, 2017, **19**, 4092–4117.

5 L. P. Tang, S. Yang, D. Liu, C. Wang, Y. Ge, L.-M. Tang, R.-L. Zhou and H. Zhang, *J. Mater. Chem. A*, 2020, **8**, 14356–14383.

6 (*a*) C. Cao, Q. Xu and Q.-L. Zhu, *Chem Catal.*, 2022, **2**, 693–723; (*b*) Y. Hou, J. Zhou, Z. He, J. Chen, M. Zhu, H. A. Wu and Y. Lu, *Nat. Commun.*, 2024, **15**, 4033; (*c*) M. Zhang, Z. Wang, X. Bo, R. Huang and D. Deng, *Angew. Chem., Int. Ed.*, 2025, **64**, e202419661.

7 B. Badhani, N. Sharma and R. Kakkar, *RSC Adv.*, 2015, **5**, 27540–27557.
8 Y. Yang, K. Sung, J. D. Lee, J. Ha, H. Kim, J. Baek, J. H. Seo, S.-J. Kim, B. Y. Lee, S. U. Son, B.-S. Kim, Y. Kim, J.-Y. Park and H.-Y. Jang, *ACS Sustainable Chem. Eng.*, 2024, **12**, 3933–3940.
9 H. S. Kim, J. Y. Jang, Y.-J. Ko, H.-Y. Jang and S. U. Son, *ACS Appl. Nano Mater.*, 2024, **7**, 12752–12760.
10 S. Petcher, D. J. Parker and T. Hasell, *Environ. Sci. Water Res. Technol.*, 2019, **5**, 2142–2149.
11 B. Wang, P. Jin, Y. Yue, S. Ji, Y. Li and H. Luo, *RSC Adv.*, 2015, **5**, 5072–5076.
12 (*a*) C. Mukherjee, D. Varghese, J. S. Krishna, T. Boominathan, R. Rakeshkumar, S. Dineshkumar, C. V. S. B. Rao and A. Sivaramkrishna, *Eur. Polym. J.*, 2023, **192**, 112068; (*b*) M. S. Kim, H. Chang, L. Zheng, Q. Yan, B. F. Pfleger, J. Klier, K. Nelson, E. L.-W. Majumder and G. W. Huber, *Chem. Rev.*, 2023, **123**, 9915–9939.
13 Y. Wang, R.-J. van Putten, A. Tietema, J. R. Parsons and G.-J. M. Gruter, *Green Chem.*, 2024, **26**, 3698–3716.
14 M. Labet and W. Thielemans, *Chem. Soc. Rev.*, 2009, **38**, 3484–3504.
15 (*a*) J. D. Lee, Y.-J. Ko, S. M. Lee, H. J. Kim and S. U. Son, *ACS Appl. Nano Mater.*, 2022, **5**, 12401–12406; (*b*) G. Yang, R. Ma, S. Zhang, Z. Liu, D. Pei, H. Jin, J. Liu and W. Du, *RSC Adv.*, 2022, **12**, 1628–1637; (*c*) C.-H. Tran, M.-W. Lee, S.-W. Park, J.-E. Jeong, S.-J. Lee, W. Song, P. Huh and I. Kim, *Catalysts*, 2021, **11**, 1033; (*d*) F. Naz, M. Ciprian, B. Mousavi, S. Chaemchuen, M. Zhu, S. Yan and F. Verpoort, *Eur. Polym. J.*, 2021, **142**, 110127; (*e*) S. J. Choi, E. H. Choi, C. Song, Y.-J. Ko, S. M. Lee, H. J. Kim, H.-Y. Jang and S. U. Son, *ACS Macro Lett.*, 2019, **8**, 687–693.
16 M. Y. Ghotbi, M. Z. Hussein, A. H. Yahaya and M. Z. A. Rahman, *Solid State Sci.*, 2009, **11**, 2125–2132.
17 D. E. Newbury, *Scanning*, 2009, **31**, 91–101.
18 N. Hirun, S. Dokmaisrijan and V. Tantishaiyakul, *Spectrochim. Acta A*, 2012, **86**, 93–100.
19 D. Ahn, J. Sun, S. Han, J. Lee, S. Jeong, S. Cha, S. Noh, H. Choi, B. Ren, H. Yoon, H. Kim and J.-J. Park, *Adv. Sci.*, 2022, **9**, 2200441.
20 Y. P. Wei, Y.-W. Zhang, J.-S. Chen, C.-J. Mao and B.-K. Jin, *Microchim. Acta*, 2020, **187**, 455.
21 S. Atta, J. Cohen, J. Kohn and A. J. Gormley, *Polym. Chem.*, 2021, **12**, 159–164.
22 F. Zhou, M. Lin, L. Li, X. Zhang, Z. Chen, Y. Li, Y. Zhao, J. Wu, G. Qian, B. Hu and W. Li, *Organometallics*, 2011, **30**, 1283–1286.
23 M. Tarnacka, A. Dzienia, P. Maksym, A. Talik, A. Zieba, R. Bielas, K. Kaminski and M. Paluch, *Macromolecules*, 2018, **51**, 4588–4597.
24 S. Klaus, M. W. Lehenmeier, E. Herdtweck, P. Deglmann, A. K. Ott and B. Rieger, *J. Am. Chem. Soc.*, 2011, **133**, 13151–13161.